

A Novel AC Technique for High Quality Porous GaN

Ainorkhilah Mahmood^{1,2,*}, Naser Mahmoud Ahmed¹, Yuhamdan Yusof¹, Yam Fong Kwong¹,
Chuah Lee Siang³, Husnen R. Abd⁴ and Zainuriah Hassan¹

¹Nano-Optoelectronics Research and Technology Laboratory, School of Physics, Universiti Sains Malaysia, 11800 Penang, Malaysia,

² Department of Applied Sciences, Universiti Teknologi MARA, 13500 Permatang Pauh, Penang, Malaysia,

³Physics Section, School of Distance Education, Universiti Sains Malaysia, 11800 Penang, Malaysia.

⁴INEE, Universiti Malaysia Perlis, 01000 Kangar, Perlis, Malaysia.

*E-mail: ainor_khilah@yahoo.com.my

Received: 2 January 2013 / *Accepted:* 29 January 2013 / *Published:* 1 April 2013

In this paper, we report the formation of porous GaN films under a novel alternating current (sine-wave a.c. (50 Hz)) photo-assisted electrochemical etching (ACPEC) conditions. The ac formed porous GaN with excellent structural and optical properties. Field emission scanning electron microscope (FESEM) micrographs indicated that the shapes of the pores are high quality hexagonal like and nano-building structures. The porous layer exhibited a substantial photoluminescence (PL) intensity enhancement with red-shifted band-edge PL peaks associated with the relaxation of compressive stress. The shift of E₂(high) to the lower frequency in Raman spectra of the porous GaN films further confirms such a stress relaxation.

Keywords: Porous GaN; Alternating current photo-assisted electrochemical etching (ACPEC); Scanning Electron Microscopy (SEM); Photoluminescence; Raman Spectroscopy.

1. INTRODUCTION

The wide band gap semiconductor GaN and related materials have been studied in preceding years due to their possible applications for optoelectronic devices operating in the spectral region from the blue to near-UV and in electronic devices such as high temperature, high power and high frequency transistor [1-3]. GaN devices are capable to operate not only at high temperature but also in hostile and harsh environments [4]. Additionally, GaN has emerged as important materials for high power electronics devices owing to its high breakdown fields [5].

Since the unearthing of porous Si shows augmented luminescence efficiency in 1990 [6], initial efforts to make porous GaN were motivated by the desire to a realize similar effect with an ultraviolet

(UV) band gap material. Porous GaN necessarily has high surface area, shift of band gap, luminescence intensity enhancement, as well as efficient photoresponse as compared to bulk. Thus, it is possible that porous GaN can be tailored to fabricate novel sensing device [7].

Several techniques are being used to prepare porous GaN; such as dry etching techniques, ion milling, chemical assisted ion beam etching, reactive ion etching and inductively-coupled plasma reactive ion etching. In general, these methods could induce surface damage, and moreover they lack the desired selectivity to the morphology, dopant and composition [8, 9]. One of the most common and feasible as a cost effective method to prepare porous GaN is the direct current (dc) photo-assisted electrochemical etching. To gain a high porosity layer, the most common technique is to use dc condition with a constant and relatively high current density. Although dramatic research has been conducted to understand the formation of porous GaN prepared by the common technique, substantial fundamental properties are still not well understood [10-16].

The idea of this study is to prepare porous GaN by a novel technique, alternating current photo-assisted electrochemical etching (ACPEC). Instead of applying the common direct current electrochemical process, alternating current is applied with a given frequency and peak voltage. The formation of porous GaN by the novel ACPEC is performed in the same electrolyte concentration (4% KOH) used in common dc constant current electrochemical etching process. Ultra-violet (UV) illumination is used to assist in the generation of electron-hole pairs, where etching proceeds through the oxidation and consequently, dissolution of the semiconductor surface. Holes play an imperative role in converting the surface atom into a higher oxidation state. The supply of holes available at the surface to participate in the oxidation reaction is greatly enhanced by the absorption of incident radiation, resulting in significantly enhanced etch rate. During the ACPEC process, the holes that are required for the process are supplied during the positive half cycle of the ac current [17]. Therefore, the correlation between the ac and dc currents, that can provide the same amount of holes can be determined by the following relation

$$\int_0^{T/2} I_{peak} \sin(2\pi ft) dt = I_{peak} T/\pi = I_{dc} \quad (1)$$

So that, the peak current can be calculated by

$$I_{peak} = I_{dc} \quad (2)$$

The current efficiency for ac condition was calculated by a weight loss method. The part of the alternating current which is actually utilized in the electrolysis is the average value or dc equivalent, denoted as I_{avg} . This can be calculated from the relation [18],

$$I_{avg} = \frac{2\sqrt{2}}{\pi} I_{rms} \quad (3)$$

where I_{rms} is the current indicated by an ac ammeter.

If Q is the quantity of electricity (where $Q = I_{avg} \times t$ and t is the time of electrolysis) used for the electrolysis, then the weight of the GaN (m') that would dissolve theoretically at 100% efficiency is

$$m' = \frac{Q A_w}{F n} \tag{4}$$

where F = Faraday; A_w = Atomic wt of GaN; n = number of electrons involved in dissolution reaction. Hence

$$m' = \frac{2 \sqrt{2} I_{rms} t A_w}{\pi n F} \tag{5}$$

Due to the nitrogen evolution, the bubble formation is observed during the ACPEC process [14]. When sine-wave ac (50 Hz) is passed across the cell containing the Pt and GaN as electrodes in a solution of (4% KOH), the following reactions may take place at the anode in the positive half-cycle depending upon the potential considerations



To the best of our knowledge, this study is the first to report on the preparation of porous GaN via the alternating current PEC (ACPEC) technique.

2. EXPERIMENT

The commercial unintentionally doped (UID) n-type GaN film grown by metalorganic chemical vapor deposition (MOCVD) on a two inch diameter sapphire (0001) substrate was used in the formation of porous GaN using the present ACPEC.

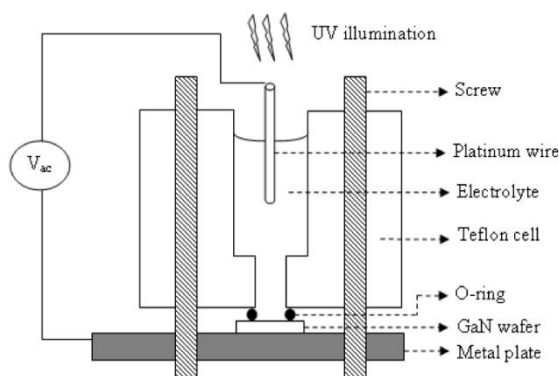


Figure 1. Schematic of alternating current photo-assisted electrochemical etching (ACPEC) apparatus

The thickness of GaN film is $3\mu\text{m}$ with carrier concentration of $\sim 6.05 \times 10^{17} \text{ cm}^{-3}$ as determined by Hall effect measurement. The wafer was then cleaved into few pieces. Prior to the metallization, the native oxide of the sample was removed in the 1:20 $\text{NH}_4\text{OH}:\text{H}_2\text{O}$ solution, followed by 1:50 $\text{HF}:\text{H}_2\text{O}$. Subsequently, boiling aqua regia (3:1 $\text{HCl}:\text{HNO}_3$) was used to etch and clean the sample.

The ac process was performed with a current density of 25 mA/cm^2 in 4% concentration of KOH electrolyte under illumination of 500 W UV for 45 and 90 minutes etch time. After chemical treatment, the samples were removed from the solution and rinsed with deionized water and dried in an ambient air. Synthesis was carried out at room temperature. Typical electrochemical cell for the generation of porous GaN are schematically shown in figure 1.

Structural properties of porous GaN were performed using field emission scanning electron microscope (FEI Nova NanoSEM 450). The optical quality of the films was studied by photoluminescence (PL) and Raman scattering. PL and Raman measurements were performed at room temperature by using JobinYvon HR800UV system, i.e. an integrated confocal micro Photoluminescence and Raman spectrometer. A He-Cd laser (325 nm) and an argon ion laser (514.5 nm) were used as an excitation source for PL and Raman measurements, respectively. For both measurements, the incident laser power was 20 mW.

3. RESULT AND DISCUSSION

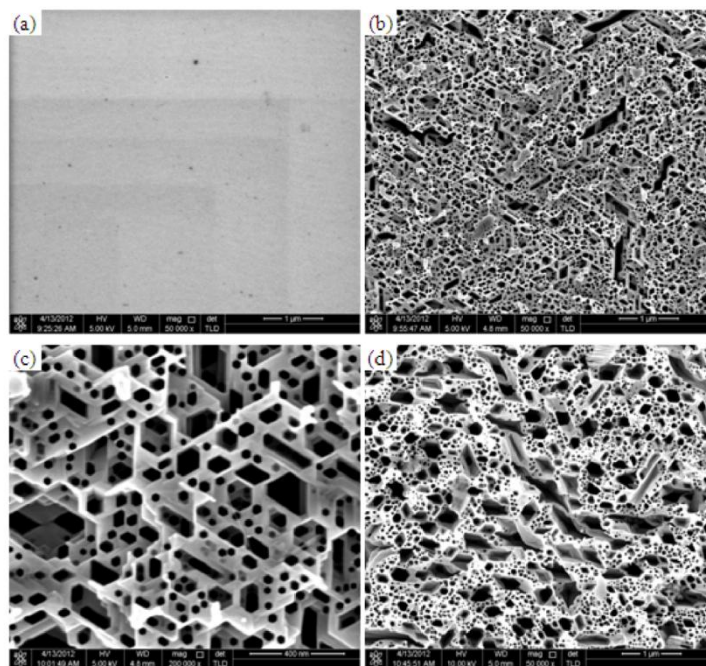


Figure 2. FESEM image of the as grown and porous GaN formed under different etching duration (a) as grown (b) 45 minutes (c) 45 minutes for high magnification, and (d) 90 minutes.

Field emission scanning electron microscopy (FESEM) images of the porous GaN samples

generated under different etching duration were shown in figure 2. FESEM images in figure 2 showed well-defined layers of pores with different sizes as a result of monocrystalline epilayer structure of GaN. The average pore size for 45 min and 90 min samples were about 35-40 nm and 55-60 nm, respectively. The average pore size varies significantly based on the quality of the starting GaN epilayers.

For 45 min sample, it appeared that etching first occurs at the centre of grain structures with the grain boundaries remain un-etched as grain boundaries are mostly defined by threading dislocation [19]. Upon removal of the materials of the grains at the top layer, subsequent etching took place at the sub-grains at the lower layer and so on, creating layered novel nano-building structures. At high magnification, it can be clearly seen from figure 2(c) that the 45 min porous sample composed of large quantities of high quality hexagonal like pores. However, when the etching duration was increased to 90 min, some of the pores merged together to form such elongated branched and also led to widen of the pores, therefore, we can observe both smaller pores and larger pores as seen in figure 2(d). When the etch rate is too large, the grain boundaries were etched significantly slower than the centre of the crystals which led to a hexagonal rough morphology. Conversely, smooth surfaces can be acquired when the etch rate in the crystal centre is slow enough so the grain boundaries were etched at an adequate rate. It means that, the final morphology of the etched surface was dependent on the relative etch rate of the centres of the grains and the grain boundaries [20].

Figure 3 illustrates the room temperature PL spectra recorded from the nano-building porous GaN etched under different durations. The PL spectrum for the as grown GaN epilayer was also shown for a comparison. The PL spectrum recorded from porous film shows a uniform PL line shape with a slight broadening toward the low-energy side. The slight broadening relative to the as grown GaN epilayer emission could be due to incorporation of impurity-induced disorder or surface defects during ACPEC [14]. The donor-acceptor pair (DAP) emission were also absent in the PL spectra for nano-building porous GaN samples. No yellow luminescence transitions were observed neither from the as grown nor the porous GaN film. The peak position, full width at half maximum (FWHM), peak shift (as compared to as grown GaN) and the intensity of near band edge PL are summarized and shown in table 1. It should be noted that the energy band gap, E_g tabulated in table 1 was calculated based on $E = hc/\lambda$, where c and λ are speed of light and wavelength, respectively. The spectra of the porous GaN samples were observed to be red shifted relative to the as grown sample. The red shift was also ascribed to the relaxation of the compressive stress in the porous samples and this relaxation can be further confirmed by Raman scattering. Similar red-shifted PL from porous GaN has been reported before [10, 12, 13, 16]. Among the samples, there is no significant difference of the peak shift, and this indicates that the change of pore size and the nano-building porous structures have little influence on the spontaneous emission of the sample. On the other hand, at room temperature, a significant enhancement of PL intensity was observed from the nano-buildings porous GaN when compared to the as grown GaN. The PL intensity for the 45 min sample was about six times greater compared to the as grown sample. As for the 90 min sample, where the pores became wider, the PL intensity enhancement was about 3 times. The improvement of PL intensity observed from the porous samples can be due to the reduction of dislocation density and extraction of strong PL by photons scattering from the sidewalls of the GaN crystallites [14], however, it could be also ascribed to the optical microcavity

effect which is inherent to porous GaN areas characterized by strong light scattering. Since the surface area per unit volume is higher in porous GaN, the larger surface area of porous GaN provides much more exposure of GaN molecules to the illumination of PL excitation lights.

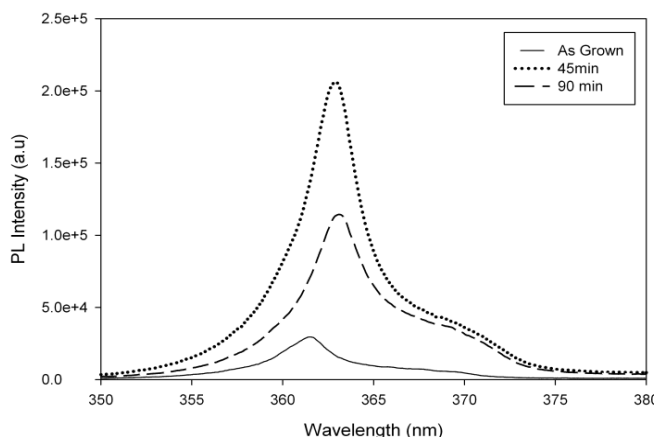


Figure 3. The near band edge PL spectra of the samples etched under different durations measured at room temperature.

In consequence, higher number of electron took part in the excitation and recombination process in porous samples compared to the lesser surface area of the as grown sample. The increase of PL line width of the porous samples which is reflected in their FWHM could be attributed to the relatively wide statistical size distribution of the pores.

Table 1. The peak position, FWHM, peak shift and relative intensity of near band edge PL of samples etched at different duration

Sample	Peak position (nm)	E _g (eV)	FWHM (nm)	Peak shift (nm)	Relative intensity
As grown	361.53	3.430	3.81	-	1.00
45 min	362.89	3.416	3.91	1.36	5.98
90 min	363.13	3.414	4.52	1.60	2.88

For appraising GaN microscopic disorder, Raman scattering is a powerful tool that can be used. Raman scattering is also effective for monitoring internal stress by measuring the frequency, polarization properties and broadening of the Raman active phonons. The Raman spectra for porous GaN and as grown samples were shown in figure 4. Raman spectra exhibited the shift of E₂(high) to the lower frequency for porous samples and followed the same trend as the PL peak shift. These revealed that stress relaxation had taken place in these samples, in which high density of pores could be found in this sample. The amount of stress relaxation can be obtained by

$$\Delta\omega_{E2} = K_R\sigma \tag{7}$$

where K_R was the proportionality factor of $4.2 \text{ cm}^{-1} \text{ GPa}^{-1}$ for hexagonal GaN and σ was the in a plane biaxial stress [21]. The shift corresponds to a relaxation of compressive stress by 0.51 GPa and 0.25 GPa in 45 min and 90 min samples, respectively. This indicated that, the amount of stress relaxation in different porous samples depends on pore size and nano-building porous GaN films with smaller pore size revealed a significant stress relaxation. Consequently, by controlling the pore diameter, we can control the amount of stress relaxation in porous GaN.

In addition, owing to multiple scattering of light and more efficient coupling of the scattered radiation due to presence of surface disorder introduced by the surface nano-building structure, there was an enhancement for the overall Raman intensity for the porous samples, and the spectral lineshape was quite similar in both porous GaN. However, the intensity enhancement was not proportional to the ACPEC durations.

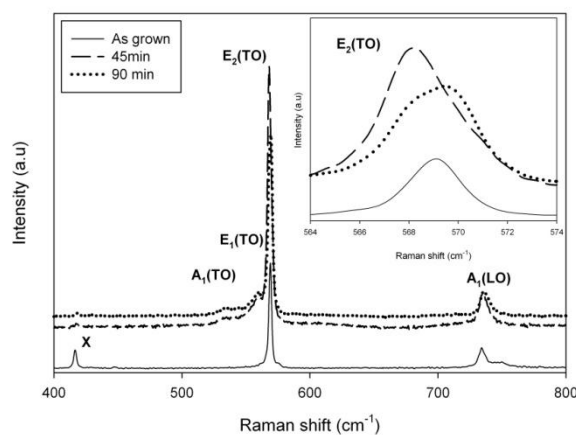


Figure 4. The Raman spectra of different samples. Inset: the observed shift for $E_2(\text{high})$ from porous film.

Table 2. Peaks position, position of E_2 (high), A_1 (TO) and E_1 (TO) of different samples obtained from Raman spectra

Sample	E_2 (high)	A_1 (TO)	E_1 (TO)
	Peak position (cm^{-1})	Peak position (cm^{-1})	Peak position (cm^{-1})
As grown	570.50	-	-
45 min	568.37	533.28	558.32
90 min	569.44	533.28	560.00

In our study, Raman scattering experiments were carried out in the $z(x, \text{unpolarized})\bar{z}$ scattering configuration, where x is the in-plane direction (perpendicular to the c axis of the hexagonal crystal). Under the Raman selection rules, $A_1(\text{LO})$ and E_2 are the only two allowed phonon modes in this scattering geometry. The spectra are dominated by strong $E_2(\text{TO})$ and $A_1(\text{LO})$ phonons near 568 and 734 cm^{-1} , which are in agreement with Raman selection rules for wurtzite GaN. From the Raman spectra, the weak features related to forbidden A_1 transverse optical (TO) and $E_1(\text{TO})$ phonon modes

were present for both 45 min and 90 min porous samples. The presence of these two peaks may be attributed to the crystal lattice disorder and to the deviation from the true backscattering geometry. For as grown sample, the exciting light with quantum energy much lower than the band gap energy of GaN penetrates into the substrate, inducing a pronounced contribution to the Raman scattering spectrum (the peak marked by cross at the corresponding curve as shown in figure 4 caused by light scattering in the sapphire substrate) [21]. Table 2 compiles the peak position of $E_2(\text{high})$, and $A_1(\text{TO})$ and $E_1(\text{TO})$ forbidden modes obtained from Raman spectra for different samples.

4. CONCLUSIONS

In summary, a novel, simple and cost-effective alternating current PEC (ACPEC) was proven to be an effective technique to form nano-porous GaN with the excellent properties. FESEM images suggested that the different etching duration had significant effect on the size of the pores. Photoluminescence (PL) measurements revealed that the near band edge peaks of all the porous samples were red shifted. Raman spectra exhibited the shift of $E_2(\text{high})$ to the lower frequency relative to the as grown sample. This indicates that it is promising to prepare high quality nano-porous GaN layer with tuneable stress. We strongly believe that further refinements of the sine-wave ac (50 Hz) electrochemical processing technologies will enhance their roles in semiconductor nanotechnology and nanoelectronics in the near future.

ACKNOWLEDGMENTS

Support from Universiti Sains Malaysia 1001/PFIZIK/814189 and UiTM Dana Kecemerlangan Research Grant 600-RMI/ST/DANA5/3/Dst (135/2011) are gratefully acknowledged.

References

1. S.C. Jain, M. Willander, J. Narayan, R. Van Overstraeten, *Journal of Applied Physics*, 87 (2000) 965-1006.
2. D. Feiler, R.S. Williams, A.A. Talin, H. Yoon, M.S. Goorsky, *Journal of Crystal Growth*, 171 (1997) 12-20.
3. G. Landwehr, A. Waag, F. Fischer, H.J. Lugauer, K. Schüll, *Physica E: Low-dimensional Systems and Nanostructures*, 3 (1998) 158-168.
4. J.-Y. Duboz, M.A. Khan, Transistors and detectors based on GaN-related materials, in: B. Gil (Ed.) *Group III Nitrides Semiconductors Compounds*, Clarendon Press, Oxford, 1998, pp. 343-390.
5. S.J. Pearton, F. Ren, A.P. Zhang, K.P. Lee, *Materials Science and Engineering: R: Reports*, 30 (2000) 55-212.
6. L.T. Canham, *Applied Physics Letters*, 57 (1990) 1046-1048.
7. X. Li, Y.-W. Kim, P.W. Bohn, I. Adesida, *Applied Physics Letters*, 80 (2002) 980-982.
8. I. Adesida, C. Youtsey, A.T. Ping, F. Khan, L.T. Romano, G. Bulman, *MRS Internet J. Nitride Semiconductor Res.*, 4S1 (1999).
9. C. Youtsey, I. Adesida, L.T. Romano, G. Bulman, *Applied Physics Letters*, 72 (1998) 560-562.
10. M. Mynbaeva, N. Bazhenov, K. Mynbaev, V. Evstropov, S.E. Sadow, Y. Koshka, Y. Melnik, *physica status solidi (b)*, 228 (2001) 589-592.

11. F.K. Yam, Z. Hassan, S.S. Ng, *Thin Solid Films*, 515 (2007) 3469-3474.
12. A. Mahmood, N.M. Ahmed, Z. Hassan, F.K. Yam, S.K.M. Bakhori, Y. Yusof, L.S. Chuah, *Advanced Materials Research*, 364 (2012) 90-94.
13. A. Mahmood, Z. Hassan, F.K. Yam, L.S. Chuah, *Optoelectron. Adv. Mater. Rapid Comm.*, 4 (2010) 1316-1320.
14. A.P. Vaipheyi, S.J. Chua, S. Tripathy, E.A. Fitzgerald, W. Liu, P. Chen, L.S. Wang, *Electrochemical Solid State Lett.*, 8 (2005) G85-G88.
15. M. Mynbaeva, A. Titkov, A. Kryganovskii, V. Ratnikov, K. Mynbaev, H. Huhtinen, R. Laiho, V. Dmitriev, *Applied Physics Letters*, 76 (2000) 1113-1115.
16. A. Mahmood, Z. Hassan, Y.F. Kwong, S.K.M. Bakhori, C.L. Siang, *AIP Conference Proceedings*, 1341 (2011) 45-47.
17. P. Allongue, V. Kieling, H. Gerischer, *Electrochimica Acta*, 40 (1995) 1353-1360.
18. S.Z. Fernandes, S.G. Mehendale, S. Venkatachalam, *J Appl Electrochem*, 10 (1980) 649-654.
19. H. Hartono, C. B.Soh, S.J. Chua, E.A. Fitzgerald, *Phys. Stat. Sol. (c)*, 4 (2007) 2572.
20. J.A. Bardwell, J.B. Webb, H. Tang, J. Fraser, S. Moisa, *Journal of Applied Physics*, 89 (2001) 4142-4149.
21. I.M. Tiginyanu, A. Sarua, G. Irmer, J. Monecke, S.M. Hubbard, D. Pavlidis, V. Valiaev, *Physical Review B*, 64 (2001) 233317.